© 2017. Published by The Company of Biologists Ltd | Journal of Experimental Biology (2017) 220, 3657-3670 doi:10.1242/jeb.161562

RESEARCH ARTICLE

A role for tight junction-associated MARVEL proteins in larval sea lamprey (*Petromyzon marinus*) osmoregulation

Dennis Kolosov[1,*], Phuong Bui[1], Andrew Donini[1], Mike P. Wilkie[2] and Scott P. Kelly[1,‡]

ABSTRACT

This study reports on tight junction-associated MARVEL proteins of larval sea lamprey (*Petromyzon marinus*) and their potential role in ammocoete osmoregulation. Two occludin isoforms (designated Ocln and Ocln-a) and a tricellulin (Tric) were identified. Transcripts encoding *ocln*, *ocln-a* and *tric* were broadly expressed in larval lamprey, with the greatest abundance of *ocln* in the gut, liver and kidney, *ocln-a* in the gill and skin, and *tric* in the kidney. Ocln and Ocln-a resolved as ∼63 kDa and ∼35 kDa MW proteins, respectively, while Tric resolved as a ∼50 kDa protein. Ocln immunolocalized to the gill vasculature and in gill mucous cells while Ocln-a localized to the gill pouch and gill epithelium. Both Ocln and Ocln-a localized in the nephron, the epidermis and the luminal side of the gut. In branchial tissue, Tric exhibited punctate localization, consistent with its presence at regions of tricellular contact. Following ion-poor water (IPW) acclimation of ammocoetes, serum [Na^+] and [Cl^-] decreased, but not [Ca^{2+}], and carcass moisture content increased. In association, Ocln abundance increased in the skin and kidney, but reduced in the gill of IPW-acclimated ammocoetes while Ocln-a abundance reduced in the kidney only. Tric abundance increased in the gill. Region-specific alterations in *ocln*, *ocln-a* and *tric* mRNA abundance were also observed in the gut. Data support a role for Ocln, Ocln-a and Tric in the osmoregulatory strategies of a basal vertebrate.

KEY WORDS: Occludin, Tricellulin, Agnathan, Osmoregulation, Epithelium, Gill

INTRODUCTION

The sea lamprey (*Petromyzon marinus* Linnaeus 1758) is an extant basal vertebrate, belonging to one of only two surviving agnathan vertebrate clades (Smith et al., 2013). Lampreys (or Petromyzontiformes) differ from members of the second extant agnathan clade, hagfishes (or Myxinoformes), because they are represented by stenohaline freshwater (FW) and euryhaline forms, whereas the hagfishes are exclusively stenohaline marine organisms (Smith et al., 2013). The life cycle of *P. marinus* involves two distinct life stages separated by a protracted period of metamorphosis. The first 3–7 years of the life cycle are spent as a comparatively sessile filter-feeding larval form called an ammocoete. Ammocoete larvae live in the substrate of rivers and streams as stenohaline FW organisms that exhibit physiological adaptations typical of other FW vertebrates (Parry, 1966). Although stenohaline, larval sea lampreys are found in FW of differing ionic strength owing to variation in drainages sources, local geochemical factors, and patterns of precipitation and evaporation (Wetzel, 1983). Following metamorphosis and after migrating to seawater (SW), *P. marinus* transform into raptorial/parasitic animals that feed on the blood and body fluids of other fishes, before returning to FW to spawn (Peek and Youson, 1979). The sea lamprey is therefore an osmo/ionoregulator that maintains comparatively stable serum ion levels in environments ranging from FW to SW, but whether they are stenohaline or euryhaline is dependent on life stage (Beamish, 1980; Zydlewski and Wilkie, 2013).

Vertebrates that reside in FW face the challenge of mitigating diffusive ion loss from ion-rich extracellular fluid to a dilute surrounding environment (Bentley, 2002). This is accomplished, in part, by deep tight junctions (TJs), which are found between epithelial cells that interface directly with water (Chasiotis et al., 2012a; Evans et al., 2005; Marshall and Grosell, 2006). These TJs, or more specifically the TJ proteins that constitute them, regulate paracellular solute movement and thereby control paracellular solute loss across tissue–water barriers such as the gill epithelium and epidermis (Chasiotis et al., 2012a; Evans et al., 2005; Marshall and Grosell, 2006; Karnaky, 2001; Kolosov et al., 2013). In addition, other epithelial tissues involved in the regulation of FW vertebrate salt and water balance, such as those of the kidney and gastrointestinal (GI) tract, possess TJs that restrict solute loss and/or contribute to the reabsorption or acquisition of salts (Kolosov et al., 2013). Recent studies on the molecular physiology of aquatic vertebrate TJs and their role in osmo/ionoregulation have revealed highly complex systems (for reviews see Chasiotis et al., 2012a; Kolosov et al., 2013). However, all reports to date have focused on derived aquatic gnathostomes, such as teleost fishes or, to a lesser extent, aquatic anurans (see Chasiotis and Kelly, 2009; Chasiotis et al., 2012a; Kolosov et al., 2013). In contrast, the molecular physiology of the agnathan TJ complex has yet to be characterized.

The TJ complex is an assembly of transmembrane and cytosolic proteins found in the apicolateral domain of vertebrate epithelial cells (Farquhar and Palade, 1963; Günzel and Fromm, 2012). These apicolateral cell-to-cell connections can occur between two adjacent epithelial cells as bicellular TJs (bTJs) or at regions of tricellular contact where tricellular TJs (tTJs) occur (Furuse et al., 2014; Günzel and Fromm, 2012). The protein composition of a TJ complex and properties of TJ proteins contribute significantly to the regulated passage of solutes across an epithelium (or epithelium region) by defining TJ permeability and/or integrity. Two important TJ proteins are occludin (OCLN) and tricellulin (TRIC), both of which are T-cell differentiation protein (MAL) and related proteins for vesicle trafficking and membrane link (MARVEL) proteins, commonly referred to as TJ-associated MARVEL proteins (Furuse et al., 2014; Raleigh et al., 2010). OCLN was the first transmembrane TJ protein described in vertebrates (Furuse et al.,

[1]Department of Biology, York University, Toronto, ON, Canada M3J 1P3.
[2]Department of Biology, Wilfrid Laurier University, Waterloo, ON, Canada N2L 3C5.
*Present address: Department of Biology, McMaster University, Hamilton, ON, Canada L8S 4K1.

‡Author for correspondence (spk@yorku.ca)

S.P.K., 0000-0002-5421-873X

Received 26 April 2017; Accepted 7 August 2017

Journal of Experimental Biology (2017) 220, 3657-3670 doi:10.1242/jeb.161562

1993), and it appears to have arisen in deuterostomes as an important structural protein (Chapman et al., 2010). OCLN/Ocln localizes at bTJs in the epithelia of mammals (Furuse et al., 1993), birds (Furuse et al., 1994), reptiles (Biazik et al., 2007), amphibians (Chen et al., 1997) and teleost fishes (Chasiotis and Kelly, 2008). Many studies have underscored the importance of OCLN/Ocln in the formation and/or maintenance of normal barrier function in different vertebrate clades under different conditions (e.g. Balda et al., 1996; Chen et al., 1997; Furuse et al., 1998; Chasiotis and Kelly, 2009; Chasiotis et al., 2012b; Kolosov et al., 2014; Krug et al., 2009). However, the precise role of OCLN/Ocln in the vertebrate epithelium is far from clear, as OCLN overexpression typically appears to reduce solute movement by enhancing barrier properties of an epithelium while a reduction in OCLN/Ocln is not always seen to have an opposite effect (for a review, see Günzel and Fromm, 2012). In contrast to OCLN, TRIC/Tric is exclusively found in the tTJ complex and has been functionally characterized only in the tissues of mammals (Ikenouchi et al., 2005; Riazuddin et al., 2006) and one species of teleost fish (Kolosov and Kelly, 2013). The loss of TRIC/Tric via transcriptional knockdown or pharmacological displacement from the tTJ complex leads to a substantial reduction in the barrier properties of diverse epithelia including the teleost fish gill epithelium (Chishti et al., 2008; Ikenouchi et al., 2005; Kolosov and Kelly, 2013; Krug et al., 2013; Riazuddin et al., 2006). Although OCLN/Ocln and TRIC/Tric play integral roles in maintaining the barrier properties of vertebrate epithelia, the work conducted on them to date has only focused on a limited number of derived vertebrate models. Nothing is known about the properties of these TJ proteins in extant basal vertebrates.

The ultrastructure of lamprey TJs (particularly in the gill) during its life cycle have been carefully described, and are known to exhibit morphological alterations associated with developmental change and life stage habitat (Peek and Youson, 1979; Bartels and Potter, 1991, 1993, 2004). These features make the sea lamprey a convenient model with which to study the role of TJ proteins in the iono/osmoregulatory physiology of an extant basal vertebrate, and in this regard it can be predicted that changes in the molecular physiology of larval sea lamprey TJs will occur in response to changes in the ionic strength of surrounding water. To address this possibility and to gain insight into the molecular physiology of the TJ complex in the sea lamprey, the present study sought to: (1) identify and characterize sea lamprey TJ-associated MARVEL proteins Ocln and Tric, and (2) consider how Ocln and Tric might contribute to osmoregulatory homeostasis of larval lamprey by examining alterations in Ocln and Tric abundance following acclimation of animals to ion-poor surroundings.

MATERIALS AND METHODS

Experimental animals

Sea lamprey (*P. marinus*) ammocoetes were captured in tributaries of the Richibucto River, New Brunswick, Canada, by pulsed DC electrofishing. Animals were transported back to Ontario in aerated coolers, and at York University, were maintained in opaque 60 litre tanks supplied with flow-through dechlorinated FW (approximate concentration in μmol l^{-1}: Na^+ 590, Cl^- 920, Ca^{2+} 760, K^+ 43; pH 7.35). Holding tank water was filled with diffusely distributed polyester stuffing (Eversoft Fibre and Foam, Toronto, ON, Canada) for thigmotaxis (Wilkie et al., 1999) and water temperature ranged from 15 to 18°C. Photoperiod was constant at 12 h:12 h light:dark and ammocoetes were fed once a week by adding a suspension of yeast (2 g per ammocoete; Red Star dry yeast, Milwaukee, WI, USA) to tank water. Animals were held under laboratory conditions for 1 month prior to any experimentation. All animal husbandry and experiments were conducted in accordance with guidelines set out by the Canadian Council of Animal Care, under the approval of the York University Animal Care Committee.

Gene identification and molecular analyses

Gene-specific primers were designed based on sea lamprey genomic information available from the Ensembl Genome Browser (http://useast.ensembl.org/index.html). The identity of annotated genes was confirmed using sequence identity comparison and NCBI BLAST searches. RNA extraction from lamprey tissues, cDNA synthesis and quantitative real-time PCR (qPCR) analysis was conducted according to previously published protocols (see below for details). PCR products employing gene-specific primers were used to sequence in full across transcripts encoding TJ proteins and these sequences were translated to protein for further analysis and custom antibody design.

Custom-synthesized antibody design and validation

Custom-synthesized antibodies were designed against epitopes in sea lamprey Ocln (CLNAELDRLPEDSAR peptide), Ocln-a (YGSRGPTGDFNAEPC peptide) and Tric (CLDHSPAPKRRPEIR peptide). Epitopes were designed away from putative post-translational modification (PTM) sites detected using NetPhosK 1.0 (http://www.cbs.dtu.dk/services/NetPhosK/). Every antibody was used with homogenates from at least two tissues (see Figs 3–5) where it was confirmed to detect a protein of appropriate molecular weight (MW). Antibodies that detected more than one band were coupled with a peptide block procedure (i.e. antibody was pre-incubated with immunization peptide in excess 1:10 ratio overnight at 4°C) in order to confirm that the antibody was recognizing the protein of interest at the appropriate MW.

Sampling of discrete organs

Ammocoetes were anaesthetized using buffered MS-222 (0.5 g l^{-1}; tricaine methasulfonate, Syndel Laboratories, Canada) and killed by spinal transection. Brain, gill, whole gut, liver, kidney and skin samples were dissected and placed in ice-cold Trizol reagent (Invitrogen Canada). Samples were frozen in liquid nitrogen, as were samples (gill and kidney, no Trizol) collected for western blot analysis. Tissues in Trizol and those for western blot analysis were stored at −80°C until use. For immunohistochemistry (IHC), gill, skin, gastrointestinal (GI) tract (anterior, middle and posterior) and kidney samples were fixed in Bouin solution (4 h at room temperature), after which Bouin solution was cleared with 70% ethanol. Fixed tissue was stored in 70% ethanol until further processing. Bouin-fixed gill samples were also used for periodic acid–Schiff (PAS) staining.

RNA extraction, cDNA synthesis and qPCR analysis

Total RNA was extracted from samples using Trizol reagent according to the manufacturer's instructions. Total RNA concentration of each sample was determined using a Multiskan Spectrum UV/Vis microplate spectrophotometer (Thermo Fisher Scientific, Nepean, ON, Canada). Total RNA (2 μg) was subjected to DNase I treatment (Amplification Grade, Invitrogen) and used for synthesis of cDNA using Super-Script III Reverse Transcriptase and Oligo(dT)12–18 primers (Invitrogen Canada).

Gene-specific optimized primer sets (see Table 1), were used to determine transcript abundance of lamprey *ocln*, *ocln-a* and *tric* by qPCR. qPCR was performed with SYBR Green I Supermix (Bio-Rad Laboratories Canada, Mississauga, ON, Canada) and a Chromo4

Detection System (CFB-3240; Bio-Rad Laboratories). The following reaction conditions were used: one cycle denaturation (95°C, 4 min), 40 cycles of: (i) denaturation (95°C, 30 s), (ii) annealing (see Table 1, 30 s) and (iii) extension (72°C, 30 s) with each qPCR run culminating in a melting curve analysis. For qPCR, elongation factor 1α (*ef-1α*) was used as a reference gene. The use of *ef-1α* as a reference gene for qPCR analysis of *ocln*, *ocln-a* and *tric* mRNA abundance was validated by statistically comparing *ef-1α* threshold cycle (C_t) values between experimental groups to confirm that *ef-1α* C_t remained constant (P>0.05) irrespective of experimental treatment.

Western blot and IHC analyses

Polyclonal rabbit anti-lamprey Ocln, Ocln-a and Tric antibodies were synthesized and obtained from GenScript (Piscataway, NJ, USA). Immunoreactivity of each custom synthesized antibody was examined by western blot analysis. The same custom synthesized antibodies were used for IHC. Western blot and IHC procedures are described in detail by Chasiotis et al. (2009) and by Chasiotis and Kelly (2008).

Western blot procedures

Samples were defrosted and disrupted in lysis buffer (10 mmol l^{-1} Tris-HCl, pH=7.5, 1 mmol l^{-1} EDTA, 0.1 mmol l^{-1} NaCl, 1 mmol l^{-1} PMSF) with 1:200 protease inhibitor cocktail (Sigma-Aldrich Canada Ltd.) using a sonicator (Misonix Sonicator XL-2000; for gill, kidney and intestine tissues) and a tissue homogenizer (PRO250, Pro Scientific; for skin samples). Disrupted samples were centrifuged at 10,000 ***g*** for 10 min at 4°C and supernatants were collected. Supernatant protein concentrations were determined using a Bradford assay protocol (Sigma-Aldrich). A standardized amount of protein from each sample was preheated in homogenization buffer (5 min at 100°C) and separated using 12% SDS-PAGE. A wet transfer (1 h at 150 mA and 100 V) was performed to move protein samples from the gel to a polyvinylidene difluoride membrane. The membrane was then blocked with a 5% skimmed milk in Tris-buffered saline with Tween (TBS-T, 10 mmol l^{-1} Tris, 150 mmol l^{-1} NaCl, 0.05% Tween-20, pH 7.4) solution for 1 h at room temperature and incubated with one of the custom synthesized rabbit anti-lamprey polyclonal antibodies. Following incubation, a horseradish peroxidase-conjugated goat anti-rabbit antibody (Bio-Rad Laboratories) was used to examine antigen reactivity with an enhanced Clarity ECL western blotting substrate (Bio-Rad Laboratories).

IHC procedures

Fixed tissue samples were dehydrated in an ascending ethanol series (70% to 100% EtOH), cleared with xylene and infiltrated with paraffin wax. Samples were then sectioned for IHC using a Leica microtome and mounted on slides. Slides were dewaxed and rehydrated in a descending ethanol series (100% to 50%, then distilled water). Na^+/K^+-ATPase (NKA) α-subunit antibody (α5; Developmental Studies Hybridoma Bank, Iowa City, IA, USA) was used to detect NKA-immunoreactive (NKA-ir) cells. Cell nuclei were stained with 4,6-diamidino-2-phenylindole (DAPI), and images were captured using an Olympus DP70 camera (Olympus Canada) coupled to a Reichert Polyvar microscope (Reichert Microscope Services).

Periodic acid–Schiff staining

PAS staining was used to identify mucous cells in the gill epithelium. Gill sections, prepared as described above (see IHC procedures), were placed into periodic acid (5 g l^{-1} periodic acid in distilled water) for 15 min and then washed (2×1 min) in distilled water. Samples were then placed into Schiff's reagent (1 g basic fuchsin/pararosniline, 2 g sodium metabisulphite and 0.3 g activated charcoal powder in a 120 ml solution composed of 100 ml distilled water and 20 ml hydrochloric acid) for 15 min and washed in distilled water for 10 min. Following this, samples were counterstained with Mayer's hemalum (50 g aluminium potassium sulfate, 1 g hematoxylin, 0.1 g sodium iodate, 1 g citric acid and 50 g chloral hydrate in 750 ml distilled water) for 2 min, washed in distilled water for 5 min and dehydrated (2×100% ethanol and xylene, 2 min each step). Slides were mounted with coverslips using Permount Mounting Medium (Fisher Scientific, Pittsburg, PA, USA) and images were captured using an Olympus DP70 camera coupled with a Reichert Polyvar microscope.

Acclimation of larval lamprey to ion-poor water

Sea lamprey ammocoetes were acclimated to ion-poor water (IPW; reverse osmosis water, approximate composition in μmol l^{-1}: Na^+ 20, Cl^- 40, Ca^{2+} 2, K^+ 0.4, pH 6.5) in 35 litre glass aquaria for a 2 week period. Control animals were held in FW in 35 litre glass aquaria. Feeding regime, photoperiod and temperature were identical to those described above.

Sampling of IPW-acclimated larval lamprey

Ammocoete larvae were anaesthetized as described previously. The caudal region was cut and blood was collected from caudal vessels into microhaematocrit tubes (Fisherbrand®, catalog no. 22-362-574). Blood was allowed to clot at room temperature for 30 min. Microhaematocrit tubes were centrifuged using a Haematokrit 20 centrifuge (Hettich Zentrifugen, 12,350 ***g*** for 5 min), following which serum was separated from packed blood cells and stored at −30°C for later analysis. Samples for qPCR and western blot analysis (i.e. gill, kidney, GI tract and skin) were collected and stored as described previously. Following the collection of all samples, a section of the remaining carcass (~1 g of the trunk region) was collected for the determination of carcass moisture content. This carcass sample was a skinless region of trunk muscle with notochord.

Sample analyses following IPW acclimation

Serum ion analysis

Serum [Na^+], [Cl^-] and [Ca^{2+}] were measured using an ion-selective microelectrode (ISME) technique as described in detail by Donini and O'Donnell (2005). Briefly, glass microcapillaries were pulled to a fine point using a Flaming-Brown pipette puller (model P97). The following ionophore cocktails were aspirated into the electrode tip and covered with polyvinylchloride (electrodes were back-filled with solutions in order to ensure ion-selective transduction of signal): Na^+ Ionophore II Cocktail A (100 mmol l^{-1} NaCl), K^+ Ionophore I Cocktail B (100 mmol l^{-1} KCl) and Ca^{2+} Ionophore I Cocktail A (100 mmol l^{-1} $CaCl_2$). A solid-state chloride electrode was used for serum chloride measurements (Donini and O'Donnell, 2005).

qPCR and western blot analysis

All procedures for qPCR and western blot followed those previously outlined.

Carcass moisture content

Samples were placed into pre-weighed tubes and dried to a constant mass at 60°C. Carcass moisture content was then calculated based on the difference between carcass wet mass and dry mass. Carcass moisture content is expressed as a percentage.

Journal of Experimental Biology (2017) 220, 3657-3670 doi:10.1242/jeb.161562

Statistics

All data are expressed as means±s.e.m. where n=number of animals. Statistical analyses were conducted using an unpaired t-test where appropriate, or a one-way ANOVA followed by a Holm–Sidak multiple comparison test using SigmaPlot (Version 11) statistical software. A fiducial limit of $P<0.05$ was observed for analysis of the effects of water ion content on the parameter measured.

RESULTS

Sea lamprey genome encodes two *ocln* genes and one *tric* gene

Two genes encoding Ocln TJ proteins (designated *ocln* and *ocln-a*) and one gene encoding the tTJ protein Tric (*tric*) were identified. These genes originated from different parts of the genome, and to fully sequence across the gene transcripts, and assemble the coding sequences so that they could be translated, multiple sets of primers were used. Sea lamprey Ocln and Ocln-a exhibited ∼38% and ∼56% sequence identity with mammalian OCLN, while sea lamprey Tric exhibited ∼53% sequence identity with mammalian TRIC. Sea lamprey Ocln, Ocln-a and Tric all mapped to the base of their respective bootstrapped phylogenetic trees (Fig. 1A). The calculated MW (in kDa) of the two Ocln proteins were determined to be quite different. Ocln was calculated to be ∼58 kDa in size (absent post-translational modifications), while Ocln-a was calculated to be ∼38 kDa (Fig. 1B). The calculated MW of sea lamprey Tric was ∼55 kDa (Fig. 1B). *In silico* analysis of protein hydrophobicity and membrane topology indicated that all three TJ proteins were tetraspanin with two extracellular loops and cytosolic N and C termini (Fig. 1C). All three proteins also possessed a MARVEL domain.

Expression profiles of *ocln*, *ocln-a* and *tric* in larval sea lamprey

Examination of different ammocoete organs (i.e. brain, gill, GI tract, liver, kidney and skin) revealed the presence of *ocln*, *ocln-a* and *tric* in each, but mRNA abundance varied. Transcript abundance of *ocln* was prominent in the GI tract, kidney and liver, and lower in the brain, gill and skin (Fig. 2A). Differences in *ocln* mRNA abundance spanned several orders of magnitude (see inset in Fig. 2A). Transcript abundance of *ocln-a* was high in the gill and skin compared with other organs (Fig. 2B). The kidney, liver and skin exhibited greater abundance of *tric* mRNA than the brain, gill and GI tract (Fig. 2C).

Immunodetection and localization of Ocln, Ocln-a and Tric in osmoregulatory organs of larval sea lamprey

Using western blot analysis with a custom-synthesized lamprey Ocln antibody, sea lamprey Ocln resolved as an immunoreactive band of ∼63 kDa (Fig. 3A). In the gill, Ocln immunoreactivity (Ocln-ir) was found in the vasculature of major and minor blood vessels in primary and secondary filaments (Fig. 3B,C). In addition, Ocln-ir cells were found at the tip of every primary gill filament as well as a layer of Ocln-ir cells lining the inside of the gill basket (Fig. 3D). These cells were identified as mucous cells using PAS staining (see inset in Fig. 3D). Ocln-ir was also observed in the nephron of the kidney, where it localized to the luminal and peritoneal sides of the kidney tubules (Fig. 3E), and the skin epidermal cells, where it localized to the basolateral membrane and to a few cells on the exterior surface of the skin (Fig. 3F). Sections of the GI tract cut tangentially revealed a typical meshwork-like staining pattern for Ocln-ir cells (Fig. 3G). In cross-section, Ocln-ir was prominent on the brush-border of the anterior, middle and posterior GI tract as well as the underlying vasculature (Fig. 3H–J). Ocln-ir seemed especially prominent in the vasculature of the anterior GI tract.

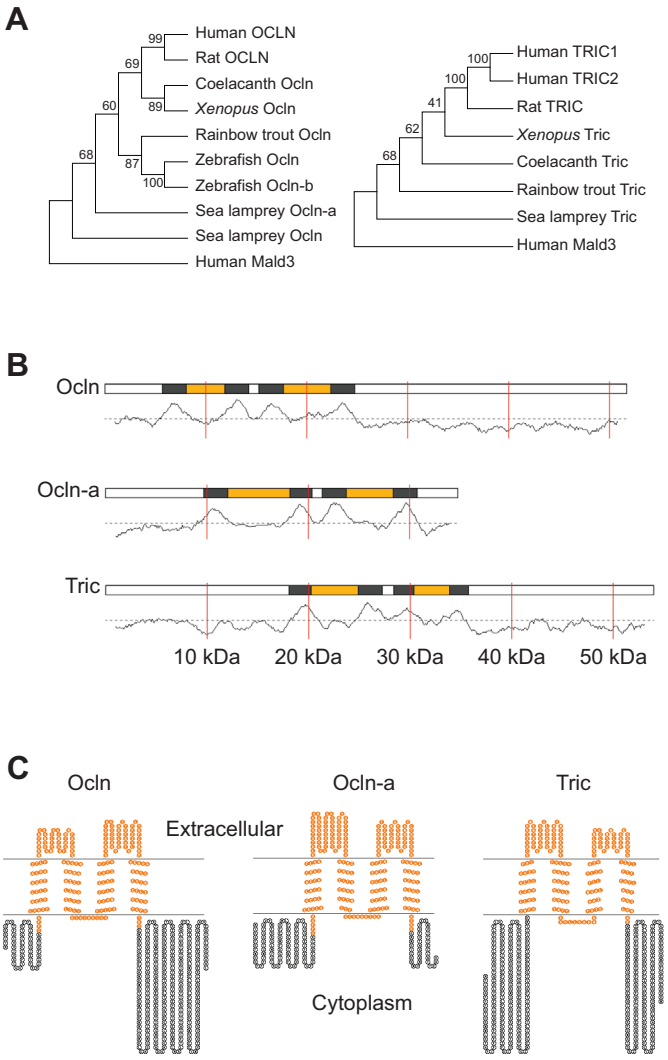

Fig. 1. Phylogeny, secondary structure and transmembrane tendency of lamprey (*Petromyzon marinus*) tight junction-associated MARVEL proteins. (A) Occludin (Ocln) and tricellulin (Tric) phylogenetic trees (relatedness between human, rat, frog, zebrafish, rainbow trout, coelacanth and sea lamprey) with human MAL and related proteins for vesicle trafficking and membrane link (MARVEL) domain-containing protein 3 (Mald3) as the outgroup. (B) Protein foldouts of lamprey (*Petromyzon marinus*) Ocln, Ocln-a and Tric demonstrate the presence of four transmembrane domains (as determined by the Kyle–Doolittle hydrophobicity score). (C) Membrane topology with MARVEL domains highlighted in orange.

Sea lamprey Ocln-a resolved as an ∼35 kDa protein by western blot analysis (Fig. 4A). Ocln-a localized to the lining of the gill pouches in a meshwork-like pattern, as well as the gill epithelium in primary and secondary filaments and the epidermal layer of the skin (Fig. 4). In addition, subcellular localization of Ocln-a in ammocoete kidney tubules was predominantly apical (in contrast to basolateral NKA-ir, see Fig. 4F). Tangential sections of GI tract revealed a meshwork-like staining pattern for Ocln-a that outlined epithelial cell TJs (Fig. 4G). Ocln-a immunolocalized to the brush-border of all three regions of the GI tract as well as the underlying vasculature (Fig. 4H-J). Ocln-a-ir seemed most prominent in the posterior GI tract brush-border.

Journal of Experimental Biology

Journal of Experimental Biology (2017) 220, 3657-3670 doi:10.1242/jeb.161562

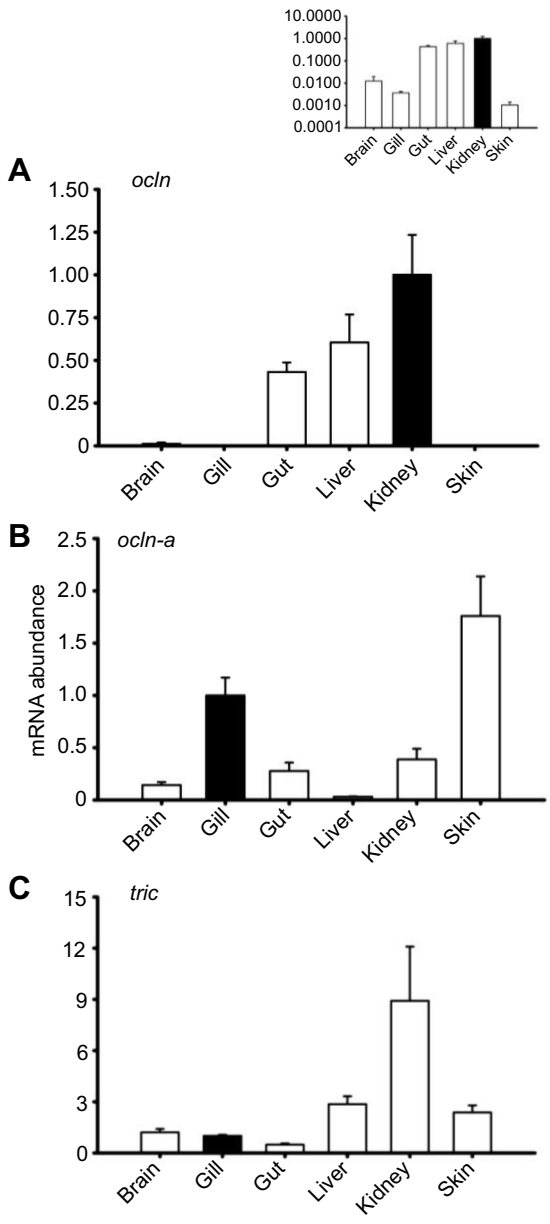

Fig. 2. Expression profiles of genes encoding lamprey (*Petromyzon marinus*) tight junction-associated MARVEL proteins. Expression profiles of (A) occludin (*ocln*), (B) occludin-a (*ocln-a*) and (C) tricellulin (*tric*) mRNA in brain, gill, gut, liver, kidney and skin of larval lamprey. Transcript abundance was determined by qPCR analysis. Elongation factor-1α (*ef-1α*) was used as a reference gene. Transcript abundance was expressed relative to an organ with a gene of interest threshold cycle value of ∼25, which was assigned a value of 1.0 (black bar). Data are expressed as means±s.e.m. (*n*=4). In A, a logarithmic *y*-axis is used for the inset graph to show that mRNA levels were detectable in all organs.

Western blot performed with custom-synthesized sea lamprey Tric antibody revealed a protein with an apparent MW of ∼50 kDa in both gill and kidney homogenates (Fig. 5). Tric IHC revealed punctate localization of Tric in epithelia lining gill pouches (Fig. 5C,D). Tric IHC in the kidney suggested that Tric presence varies in different tubule regions – one with diffuse Tric-ir throughout the tubule and another with punctate Tric-ir in cell-cell contacts facing the tubular lumen (Fig. 5E-G).

IPW acclimation of sea lamprey ammocoetes

Systemic endpoints of salt and water balance

Acclimation of ammocoetes to IPW for 2 weeks resulted in a decrease in serum [Na^+] and [Cl^-] (Fig. 6A). However, acclimation to IPW had no significant effect on serum [Ca^{2+}] (Fig. 6A). Following IPW acclimation, a significant increase in carcass moisture content was observed (Fig. 6B).

Organ-specific alterations in the abundance of Ocln, Ocln-a and Tric

Gill

Following IPW acclimation, *ocln* and Ocln abundance decreased in gill tissue while *ocln-a* and Ocln-a abundance did not significantly differ from that of control animals held in FW (Fig. 7A,B). In addition, mRNA abundance of *ocln* was two to three orders of magnitude lower than that of *ocln-a* in the gills of sea lamprey ammocoetes (data not shown). In contrast, *tric* and Tric exhibited an increase in abundance in the gill of IPW-acclimated ammocoete larvae versus those held in FW (Fig. 7A,B).

Skin

In the skin of larval lamprey, *ocln-a* was also two to three orders of magnitude more abundant than *ocln* (data not shown), and *ocln-a* as well as Ocln-a abundance were not significantly altered by IPW acclimation (Fig. 7C,D). Similarly, no significant difference occurred between skin *ocln* transcript abundance of FW- and IPW-acclimated animals, but Ocln protein abundance was significantly elevated in IPW-acclimated animals (Fig. 7D). Skin Tric was unaltered by IPW acclimation but *tric* mRNA was elevated.

Kidney

Transcript abundance of *ocln* increased ∼15-fold in the kidney of sea lamprey ammocoetes acclimated to IPW (Fig. 8A). These alterations in transcript abundance occurred in conjunction with a significant increase in Ocln protein abundance (Fig. 8B). In contrast, *ocln-a* mRNA abundance remained unaltered while protein abundance significantly decreased (Fig. 8A,B). In kidney tissue, *tric* as well as Tric were unaltered by IPW acclimation (Fig. 8). Similar to gill and skin, kidney *ocln* abundance was two to three orders of magnitude lower than *ocln-a* (data not shown).

GI tract

When comparing *ocln* and *ocln-a* transcript abundance in specific regions of the GI tract, it was observed that *ocln* exhibited either equal or greater abundance than *ocln-a* in the anterior and middle GI tract (data not shown). However, in the posterior GI tract, *ocln-a* mRNA abundance was greater than *ocln*. When considering the spatial distribution of *ocln* and *ocln-a* along the GI tract, it was observed that *ocln* exhibited a modest but significant elevation in abundance in the middle region of the GI tract, versus the anterior and posterior (Fig. 9A). In contrast, *ocln-a* was most abundant in the posterior GI tract (Fig. 9A). Similarly, *tric* mRNA exhibited a stepwise increase in abundance from anterior to posterior GI tract, resulting in greatest abundance in the posterior (Fig. 9A).

Following IPW acclimation, there were no significant alterations in *ocln*, *ocln-a* or *tric* mRNA abundance in the anterior GI tract (Fig. 9B). In the middle GI tract, *ocln* abundance significantly decreased while *ocln-a* was unaltered and *tric* increased (Fig. 9C). In the posterior GI tract, *ocln* mRNA abundance also decreased in IPW-acclimated fish, but *ocln-a* and *tric* were unaltered (Fig. 9D). Alterations in Ocln, Ocln-a and Tric protein abundance were not measured following IPW acclimation because of limitations in tissue availability.

Journal of Experimental Biology (2017) 220, 3657-3670 doi:10.1242/jeb.161562

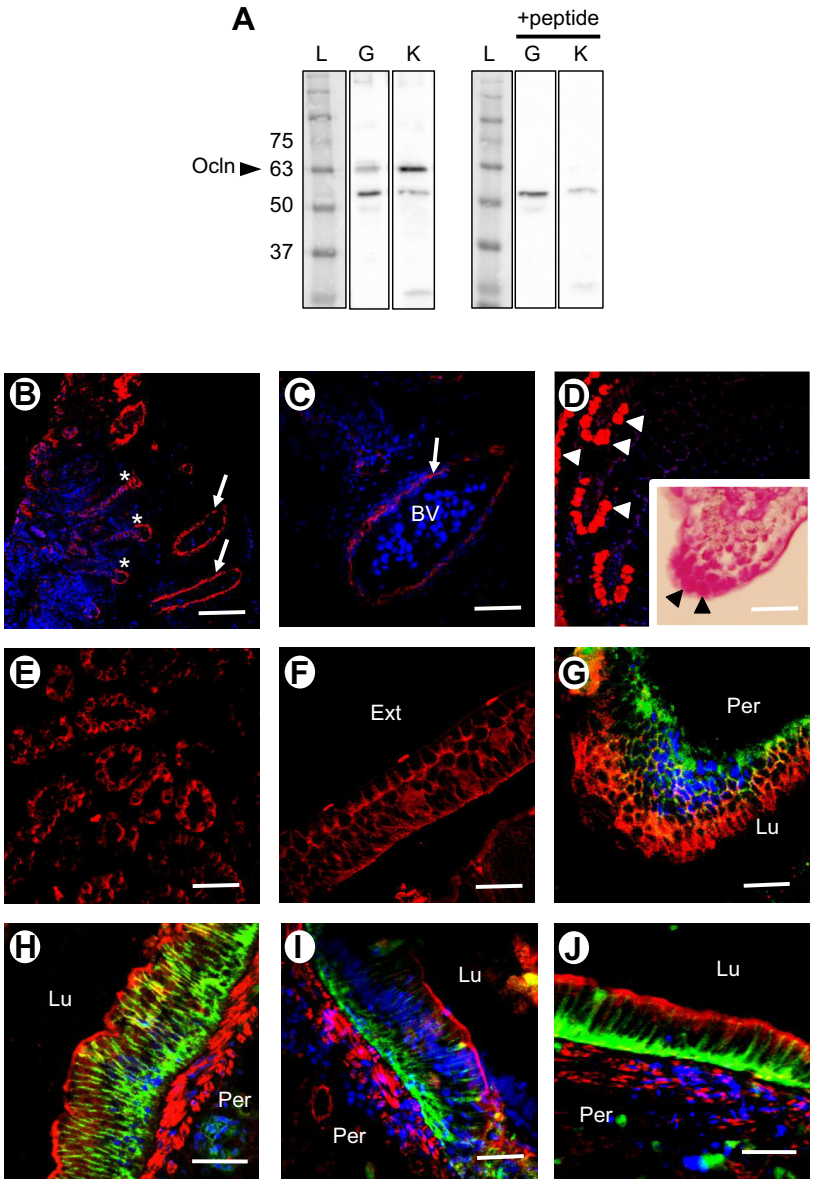

Fig. 3. Immunodetection and localization of lamprey (*Petromyzon marinus*) occludin (Ocln). Ocln was detected in larval lamprey by (A) western blot analysis and (B–J) fluorescent immunohistochemistry. In B–J, red indicates Ocln immunoreactivity (Ocln-ir), green indicates Na^+/K^+-ATPase (NKA)-ir and blue indicates 4,6-diamidino-2-phenylindole (DAPI) staining of nuclei. Western blot revealed a single immunoreactive band, blocked by a peptide pre-absorption procedure (+peptide), which resolved at ~63 kDa in gill (G) and kidney (K) homogenates (L, ladder). Ocln immunolocalized to the vasculature in the primary (white arrows) and secondary (asterisks) gill filaments (B,C), as well as (D) cells lining gill pouches and on the tip of the primary gill filaments (indicated by white arrowheads). Periodic acid–Schiff (PAS) staining identified cells located at the tip of primary gill filaments as mucous cells (see D inset, indicated by black arrowheads). (E) Ocln-ir in the kidney indicated the presence of Ocln all around tubular epithelial cells. (F) Ocln localization in the epidermal layer of the integument. Tangential sections of the gastrointestinal (GI) tract revealed a meshwork Ocln-ir pattern in the subapical region of columnar epithelial cells (G) and separate basolateral NKA-ir. In cross-sections of (H) anterior, (I) middle and (J) posterior GI tract, Ocln-ir was apical and NKA-ir basolateral. Ocln-ir was also found in the GI tract vasculature (H–J). Scale bars: (B) 50 μm, (C–J) 25 μm. BV, blood vessel; Ext, exterior; Lu, lumen; Per, peritoneal side.

DISCUSSION

Overview

Three TJ-associated MARVEL proteins – two Ocln isoforms (Ocln and Ocln-a) and a Tric – were identified in the sea lamprey. Each MARVEL domain-containing protein mapped to the base of its phylogenetic tree and genes encoding each identified protein exhibited broad expression patterns in larval lamprey organs, albeit at different levels of abundance. The two Ocln isoforms (Ocln and Ocln-a) differed in size, exhibited different patterns of localization in organs such as the gill, skin and kidney, and in these organs, Ocln and Ocln-a responded differently to IPW acclimation. Specifically, Ocln exhibited altered protein abundance in several iono/osmoregulatory organs following IPW acclimation, while Ocln-a abundance altered only in the kidney. This would suggest that of the two isoforms, Ocln may be the more dynamic regulatory protein in lamprey tissue, which would be consistent with the elongated C-terminal tail of Ocln versus Ocln-a (e.g. for post-translational modifications). In the gill and kidney, Tric localization was consistent with its presence in regions of tricellular contact between epithelial cells, but in the kidney some cells exhibited diffuse intracellular Tric presence. Protein and/or transcript abundance of Tric/*tric* increased in response to IPW acclimation in the gill, skin and middle region of the GI tract, but not the kidney. This suggests that in response to the environmental perturbation of IPW acclimation, alterations in Tric abundance of externally exposed epithelia may contribute to the maintenance of osmotic homeostasis. Taken together, the results of the present study support the idea that TJ-associated MARVEL proteins contribute to the integrity of epithelial barriers in the Petromyzontiformes, and that organ-specific adjustments in their abundance help to maintain iono/osmoregulatory homeostasis in pre-metamorphic lamprey.

Characterization of Ocln, Ocln-a and Tric in larval sea lamprey

The two Ocln isoforms and Tric found in sea lamprey share membrane topology with OCLN/Ocln and TRIC/Tric of other vertebrates. However, all three proteins were smaller than the OCLN/Ocln and TRIC/Tric of more derived vertebrates. Lamprey Ocln and Ocln-a possessed MWs of ~63 and ~35 kDa, respectively, which are lower than the typical MWs reported for vertebrate Oclns, including

Journal of Experimental Biology (2017) 220, 3657-3670 doi:10.1242/jeb.161562

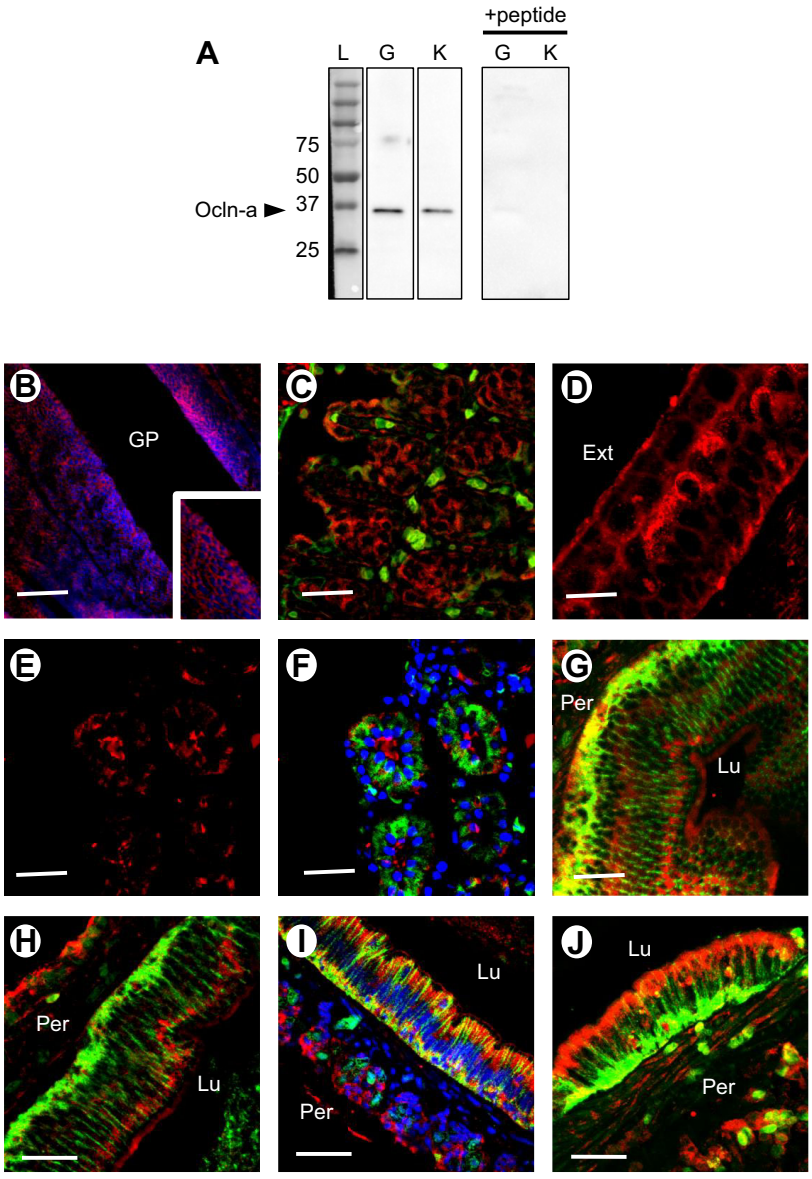

Fig. 4. Immunodetection and localization of lamprey (*Petromyzon marinus*) occludin-a (Ocln-a). Ocln-a was detected in larval lamprey by (A) western blot analysis and (B–J) fluorescent immunohistochemistry. In B–J, red indicates Ocln-a immunoreactivity (Ocln-a-ir), green indicates Na^+/K^+-ATPase (NKA)-ir and blue indicates 4,6-diamidino-2-phenylindole (DAPI) staining of nuclei. Western blot analysis revealed a single immunoreactive band, blocked by a peptide pre-absorption procedure (+peptide), which resolved at ~35 kDa in gill (G) and kidney (K) homogenates (L, ladder). In B, Ocln-a can be seen localizing to the layer of cells lining gill pouches, and in C, to epithelial cells in the primary and secondary gill filaments. (D) Ocln-a-ir in the epidermis of the integument. (E,F) Localization of Ocln-a in the kidney tubules was concentrated in the apical membrane of epithelial cells facing the lumen. Tangential sections of the GI tract revealed a meshwork pattern of Ocln-a-ir in the subapical region of columnar epithelial cells (G) and separate basolateral NKA-ir. In cross-sections of (H) anterior, (I) middle and (J) posterior GI tract, Ocln-a-ir was apical and NKA-ir basolateral. Scale bars: (B) 50 μm, (C,E–J) 25 μm, (D) 35 μm. Ext, exterior; Lu, lumen; Per, peritoneal side.

those of other fishes (i.e. ~65–70 kDa) (Furuse et al., 1993; Saitou et al., 1997; Feldman et al., 2005; Chasiotis and Kelly, 2008; Chasiotis et al., 2009, 2010, 2012a). Sea lamprey Tric possessed a MW of ~50 kDa, which is also smaller than the MW of ~70 kDa described in mammals and at least one species of teleost fish (Ikenouchi et al., 2005; Raleigh et al., 2010; Kolosov and Kelly, 2013). When the transmembrane tetraspanin MARVEL domain is taken into account, the smaller size of these TJ proteins in lamprey leaves much less protein span in the cytoplasmic N and C termini for regulatory interactions and PTM. This may indicate differences in how the proteins are regulated in basal versus derived vertebrates. For example, studies on human OCLN have demonstrated that PTM of the C-terminal cytoplasmic tail is responsible for its regulation in TJ assembly and disassembly via interaction with scaffolding TJ proteins (Dörfel et al., 2013). Interestingly, this domain was almost entirely missing from sea lamprey Ocln-a (see Fig. 1C). Ocln-a was also the sea lamprey Ocln isoform that did not respond transcriptionally to IPW acclimation in any of the tissues examined (see Figs 7–9). Therefore, it is possible that Ocln-a is a molecular component of the sea lamprey TJ complex that contributes to the integrity of bicellular junctions by being incorporated early during development and staying, for the most part, quiescent in the face of environmental perturbation. In contrast, the larger lamprey Ocln isoform (i.e. Ocln) possessed a far longer C-terminal tail than Ocln-a. If this, in turn, presents more opportunity for regulatory interactions and PTM, this could account for *ocln*/Ocln abundance being more pliant to environmental change. But it should also be noted that Ocln exhibited a much lower sequence identity to derived vertebrate Ocln than Ocln-a (i.e. ~38% versus ~56% sequence identity to mammalian Ocln).

The membrane topology and subcellular localization of lamprey Tric appeared to be in line with previous observations of this tTJ protein in other vertebrate species. However, *tric* mRNA abundance in different ammocoete organs revealed a pattern where abundance was greatest in the kidney. This is different from the *tric* expression pattern observed in rainbow trout, but it is similar to the pattern of expression in the mouse (Ikenouchi et al., 2005; Raleigh et al., 2010; Kolosov and Kelly, 2013).

Journal of Experimental Biology (2017) 220, 3657-3670 doi:10.1242/jeb.161562

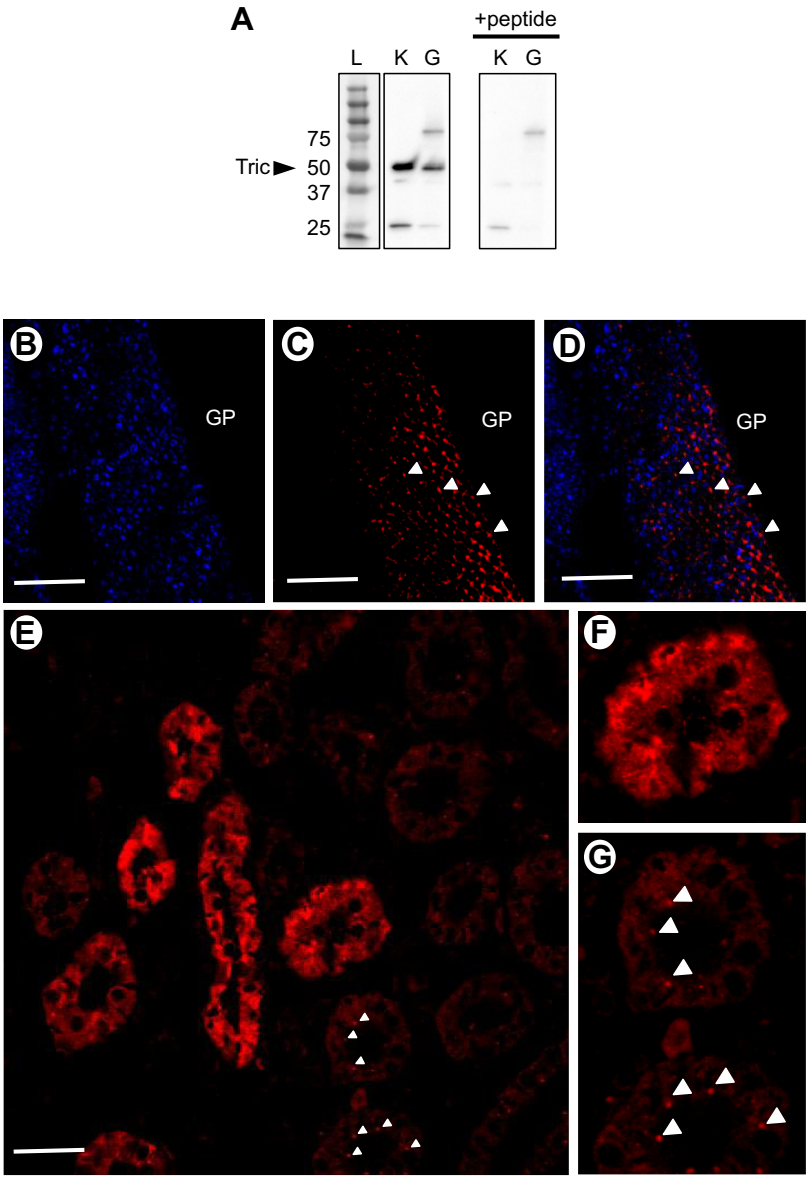

Fig. 5. Immunodetection and localization of lamprey (*Petromyzon marinus*) tricellulin (Tric). Tric was detected in larval lamprey by (A) western blot analysis and (B–G) fluorescent immunohistochemistry. In B–G, red indicates Tric immunoreactivity (Tric-ir) and blue indicates 4,6-diamidino-2-phenylindole (DAPI) staining of nuclei. (A) Western blot analysis revealed a single immunoreactive band, blocked by a peptide pre-absorption procedure (+peptide), which resolved at ~50 kDa in gill (G) and kidney (K) homogenates (L, ladder). (B) DAPI staining of nuclei in the gill pouches; (C) Tric-ir in the same region. B and C are merged in D to reveal Tric-ir at focal points (see white arrowheads) which are consistent with localization in regions of epithelial cell tricellular contact. Tric-ir in the kidney of larval sea lamprey (E) revealed both cellular localization as well as Tric-ir at focal points in the subapical domain (see white arrowheads). These patterns of Tric-ir can be seen in magnified images (F and G), and in the latter white arrowheads point to focal points of Tric-ir. Scale bars: (B–D) 25 μm, (E) 250 μm. GP, gill pouch.

Immunolocalization of Ocln, Ocln-a and Tric in larval sea lamprey

The two Ocln isoforms identified in sea lamprey exhibited patterns of localization that often differed between organs, but in some cases overlapped. For example, Ocln-a immunolocalization was observed in sea lamprey gill epithelial cells (Fig. 4B,C), whereas Ocln localized primarily in the gill vasculature and in mucous cells (Fig. 3B–D). In the goldfish gill, Ocln localized to epithelial cells as well as cells of the vasculature (Chasiotis and Kelly, 2008). Furthermore, in goldfish, Ocln did not localize in mucous cells (Chasiotis and Kelly, 2008). Therefore, in gill tissue there appear to be some differences between basal and derived aquatic vertebrates. In contrast, both Ocln and Ocln-a appeared in the skin as a meshwork around epithelial cells exposed to the surrounding water as well as in the deeper layers of the tissue.

Table 1. qPCR primers, annealing temperatures, amplicon sizes and GenBank accession numbers for sea lamprey tight junction (TJ)-associated MARVEL proteins and elongation factor-1

TJ protein	Gene	Primer sequence (5′ to 3′)	Annealing temperature (°C)	Amplicon size (bp)	GenBank accession no.
Occludin-a	*ocln-a*	F: ACCTCATCACCATCATCTG R: ACCAGCATAAAGCCACAC	54	247	KU721850
Occludin	*ocln*	F: CTACACCACAGAGCCCGAGT R: GAGAGCCGCACCTTCAGC	60	321	KU721849
Tricellulin	*tric*	F: CACATCCCCAAGCCTCTG R: CCACTCGCTCCATCTCCTG	60	226	KU721851
Elongation factor 1α	*ef-1α*	F: GTGGGTCGTGTTGAGACTGG R: GGTCGTTCTTGCTGTCAC	60	208	KU726618

Journal of Experimental Biology

Journal of Experimental Biology (2017) 220, 3657-3670 doi:10.1242/jeb.161562

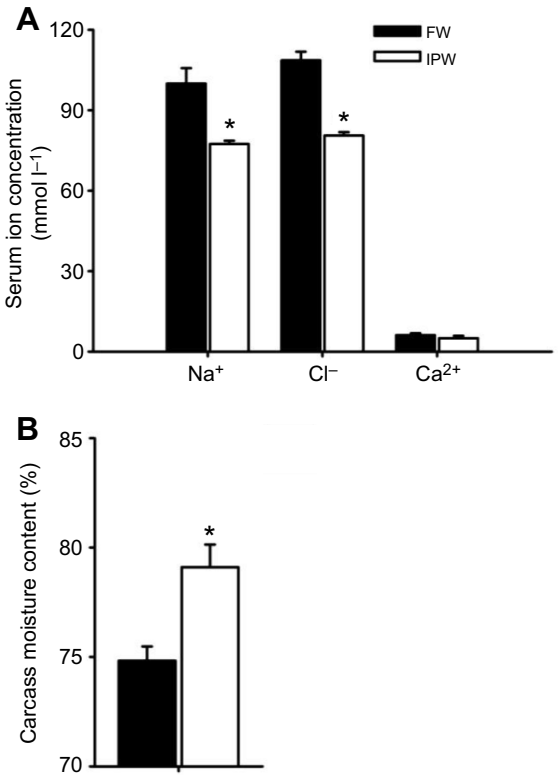

Fig. 6. Effect of ion-poor water (IPW) acclimation on systemic endpoints of salt and water balance in larval lamprey (*Petromyzon marinus*). Measured levels of (A) serum [Na^+], [Cl^-] and [Ca^{2+}] and (B) carcass moisture content of larval lamprey are shown. Data are presented as means±s.e.m. (n=10). An asterisk denotes a significant difference (P≤0.05) between freshwater (FW) control and IPW-acclimated animals as determined by an unpaired t-test.

Ocln and Ocln-a immunolocalization patterns in the larval lamprey kidney were also quite different from one another. In renal tissue, Ocln-a localized to regions of cell-to-cell contact at the tubular lumen, while Ocln was found to exhibit a general cellular staining pattern that was not restricted to regions of cell-to-cell contact in the tubular epithelium. The kidney of larval ammocoetes is heavily compartmentalized and regionalized with each pronephros containing, on average, five nephrostomes (Kluge and Fischer, 1991). The inside of the nephrostome is lined with tubular epithelium, while the outside is lined with peritoneal epithelium (Kluge and Fischer, 1991). It is possible that while Ocln-a localizes primarily to the tubular epithelium luminal border, Ocln is found in both peritoneal and tubular epithelium. Spatial differences in the localization of Ocln isoforms within renal tissue of FW larval lamprey are consistent with observations of Ocln-ir in renal tissue of at least one species of FW teleost fish (goldfish) as well as a fully aquatic FW amphibian (*Xenopus*) (Chasiotis and Kelly, 2008, 2009). In these derived FW aquatic organisms, Ocln has been shown to localize to the luminal border of the nephron distal tubule and collecting duct, but Ocln-ir is absent from the proximal tubule (Chasiotis and Kelly, 2008, 2009). These observations suggest that Ocln and Ocln-a will play region-specific roles in their contribution to nephron barrier properties in both basal and derived aquatic vertebrates.

In the GI tract, Ocln-a and Ocln both localize to the luminal side of epithelial cells in anterior, middle and posterior regions. GI tract Ocln- and Ocln-a-ir exhibited a typical honeycomb appearance when a tangential section was present. This is consistent with Ocln-ir in the intestinal enterocytes of other FW aquatic vertebrates (Chasiotis and Kelly, 2008, 2009). However, Ocln- and Ocln-a-ir were distinct in the vasculature underlying the intestinal epithelium, and prominent Ocln-ir has not been reported in the GI tract of other aquatic vertebrates (Chasiotis and Kelly, 2008, 2009). The localization of Tric in the ammocoete branchial region and in renal tissue was in line with previous findings that have described Tric at regions of tricellular contact in vertebrate epithelia (Ikenouchi et al., 2005; Krug et al., 2009; Korompay et al., 2012; Kolosov and Kelly, 2013). However, the tTJ represents a small area of any whole tissue preparation, and successful detection of Tric at tTJ contact points depends heavily on the optical sectioning of the sample in the right plane. This is especially evident in the kidney, where punctate localization of Tric (coinciding with the highest transcript abundance; see Fig. 2C) was evident in one group of tubules, while another demonstrated diffuse cytoplasmic localization of Tric. The functional properties of Ocln and Tric have yet to be detailed in the GI tract and kidney of aquatic vertebrates, but based on the immunolocalization observations, some functional overlap should be expected between basal and derived aquatic vertebrates.

IPW acclimation of larval sea lamprey

Acclimation of FW fishes to IPW magnifies the challenge of maintaining salt and water balance in hypo-osmotic surroundings. This is because the difficulties associated with hyper-osmoregulation involve balancing new ion acquisition while abating obligatory (passive) ion loss. Both of these problems, as well as the physiological, morphological, cellular and molecular processes that control them, intensify in IPW (e.g. Perry and Laurent, 1989; Chasiotis et al., 2009, 2012b; Chen et al., 2016; Kolosov and Kelly, 2016). Molecular mechanisms that help to mitigate paracellular ion loss across osmo/ionoregulatory epithelia are only now being uncovered (for reviews, see Chasiotis et al., 2012a; Kolosov et al., 2013). However, studies on derived fishes have shown that acclimation or exposure to IPW modulates select components of the TJ complex and alters paracellular permeability across ionoregulatory epithelia (Duffy et al., 2011; Chasiotis et al., 2012a; Chen et al., 2016; Kolosov and Kelly, 2016). Because lamprey larvae deal with life in FW in much the same way as derived fishes, acclimation to IPW will likely require modulation of the TJ complex.

Salt and water balance in IPW-acclimated larval sea lamprey

Acclimation of ammocoetes to IPW resulted in a significant reduction in serum [Na^+] and [Cl^-], but not serum [Ca^{2+}]. In addition to this, carcass moisture content was elevated, indicating increased tissue hydration. These changes are consistent with the challenge of acclimation to an ion-deficient medium within which lamprey ammocoetes have been documented to experience greater ion loss (Morris, 1980), as well as the observations of Hardisty (1956), who reported a reduction in serum [Cl^-] of adult and larval lamprey (*Lampetra planerii*) acclimated to distilled water. In teleost fishes abruptly exposed or acclimated to IPW, reductions in serum [Na^+] and [Cl^-] and increased muscle moisture content are also typically observed (e.g. Chasiotis et al., 2009; Duffy et al., 2011; Kolosov and Kelly, 2016). Reduced serum ion levels in IPW-acclimated lamprey larvae suggest that ammocoetes inhabiting ion-poor habitats may have a reduced capacity to deal with ionic imbalance and this should be considered relevant from a lamprey management perspective.

Journal of Experimental Biology (2017) 220, 3657-3670 doi:10.1242/jeb.161562

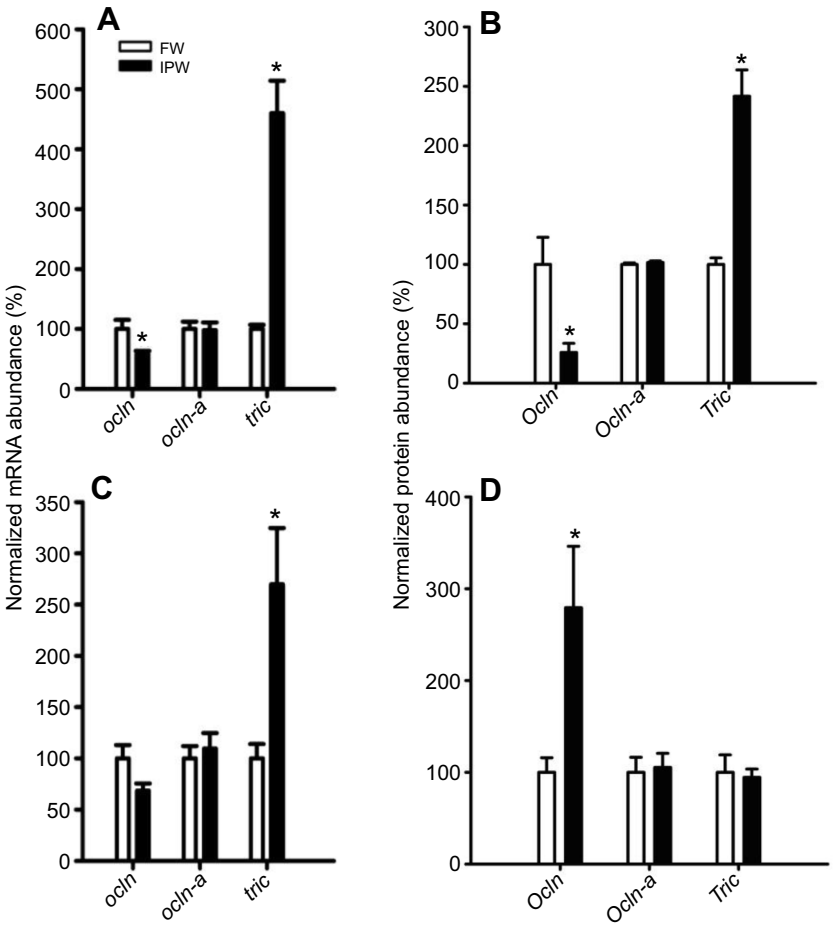

Fig. 7. Effect of IPW acclimation on the abundance of tight junction-associated MARVEL proteins in the gill and skin of larval sea lamprey (*Petromyzon marinus*). (A) Gill mRNA and (B) gill protein abundance of occludin (*ocln*/Ocln), occludin-a (*ocln-a*/Ocln-a) and tricellulin (*tric*/Tric). (C) Skin mRNA and (D) skin protein abundance of *ocln*/Ocln, *ocln-a*/Ocln-a and *tric*/Tric. Data are presented as means±s.e.m. (n=8 or 10). An asterisk denotes a significant difference ($P \leq 0.05$) between FW control and IPW-acclimated animals as determined by an unpaired t-test.

Organ-specific changes in TJ-associated MARVEL proteins following IPW acclimation of larval lamprey

Ammocoete gill

Gill *ocln*/Ocln abundance decreased in response to 14 days of IPW acclimation of ammocoetes, while gill *ocln-a*/Ocln-a abundance did not change. When goldfish, which like ammocoetes are FW and stenohaline organisms, are acclimated to IPW for 14 days, mRNA and protein abundance of Ocln has been reported to increase in the gill (Chasiotis et al., 2009, 2012b). In goldfish, this was proposed to be in line with the barrier-forming properties of Ocln in the gill epithelium (Chasiotis et al., 2012b). For this reason, it was surprising that ammocoete gill Ocln and Ocln-a, which collectively exhibit a pattern of localization in the ammocoete gill that is similar to the pattern of Ocln in goldfish, did not comparably respond to IPW. However, there is evidence to suggest that alterations in teleost fish gill *ocln*/Ocln abundance are sensitive to the duration of IPW exposure. For example, rainbow trout gill *ocln* abundance was not altered 24 h following IPW exposure (Kolosov and Kelly, 2016; Chen et al., 2016) and although gill Ocln abundance increased in goldfish acclimated to IPW for 14 days, it was not different from that of control animals (held in regular FW) from 3 h to 5 days (Chasiotis et al., 2009). Future time-course

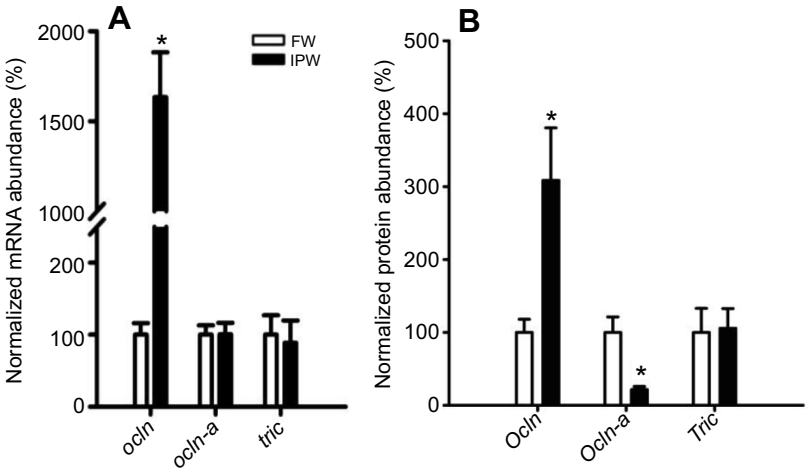

Fig. 8. Effect of IPW acclimation on the abundance of tight junction-associated MARVEL proteins in the kidney of larval sea lamprey (*Petromyzon marinus*). Kidney (A) mRNA and (B) protein abundance of occludin (*ocln*/Ocln), occludin-a (*ocln-a*/Ocln-a) and tricellulin (*tric*/Tric) are shown. Data are presented as means±s.e.m. (n=8 or 10). An asterisk denotes significant difference ($P \leq 0.05$) between FW control and IPW-acclimated animals as determined by an unpaired t-test.

Journal of Experimental Biology

Journal of Experimental Biology (2017) 220, 3657-3670 doi:10.1242/jeb.161562

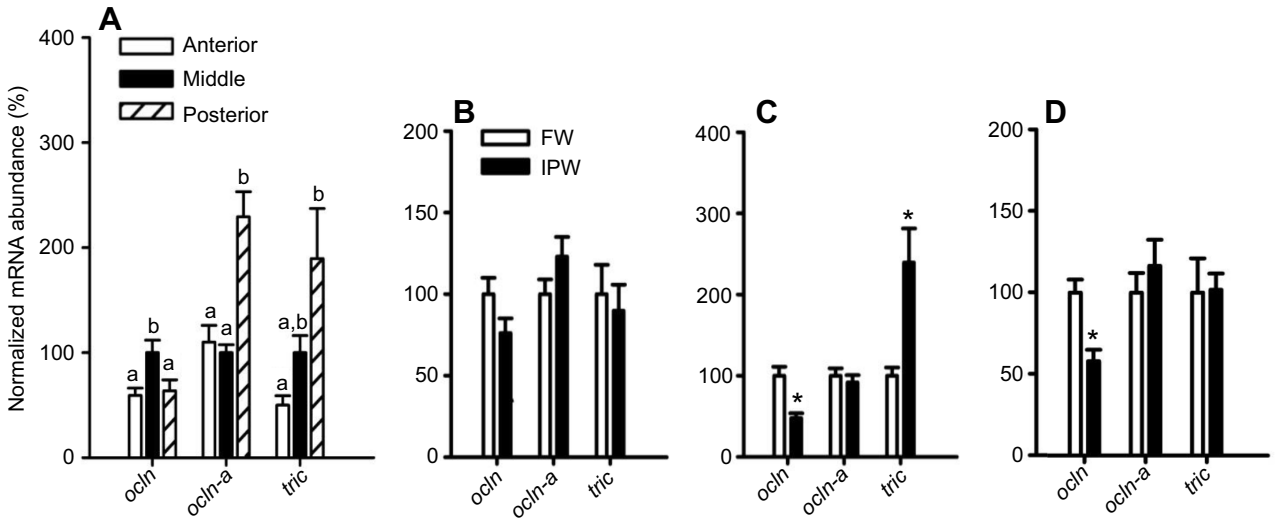

Fig. 9. Spatial differences and the effect of IPW acclimation on transcript abundance of tight junction-associated MARVEL proteins in the GI tract of larval sea lamprey (*Petromyzon marinus*). (A) Transcript abundance of occludin (*ocln*), occludin-a (*ocln-a*) and tricellulin (*tric*) along the GI tract from anterior to posterior and (B–D) the effect of IPW acclimation on mRNA abundance in the (B) anterior, (C) middle and (D) posterior GI tract. Data are presented as means±s.e.m. (n=8 or 10). In A, different lowercase letters indicate a significant difference (P≤0.05) in transcript abundance between different GI tract regions as determined by a one-way ANOVA. In B–D, an asterisk denotes a significant difference (P≤0.05) between FW control and IPW-acclimated animals as determined by an unpaired t-test.

studies would be able to examine changes in ammocoete gill *ocln*/Ocln more broadly and possibly pinpoint changes in *ocln-a*/Ocln-a abundance, if changes in this isoform do occur. It was also notable that lamprey Ocln-ir was observed in mucous cells on primary gill filament tips. This suggests that changes in mucous cell number or size may influence measurements of gill Ocln abundance in ammocoete gill. Therefore, while some data suggest that Ocln isoforms play a role in gill barrier function in larval lamprey, the specific role of different Ocln isoforms requires further study using tools such as those used to elucidate the function of Ocln in the gill epithelium of derived fishes (Chasiotis et al., 2009, 2012b; Kelly and Chasiotis, 2011).

In the gill of ammocoetes acclimated to IPW, both *tric* and Tric abundance increased. Increased protein abundance of Tric in the ammocoete gill is in line with the currently proposed contribution of Tric to teleost gill epithelium barrier function (Kolosov and Kelly, 2013). More specifically, in a primary cultured teleost fish gill epithelium model, Tric abundance increased in association with a corticosteroid-induced reduction in gill epithelium permeability, and pharmacological removal of Tric from regions of tricellular contact in the model gill significantly increased epithelium permeability (Kolosov and Kelly, 2013). In line with both of these observations, a solute barrier function for TRIC has also been demonstrated in mammalian systems, including epidermal, nasal, GI and cochlear epithelia (Ikenouchi et al., 2005; Riazuddin et al., 2006; Krug et al., 2013; Schlüter et al., 2007; Ohkuni et al., 2009).

Ammocoete skin

A link between skin barrier function in salt and water balance and the composition and/or abundance of epidermal TJ proteins has been suggested for teleost fishes residing in FW, SW and/or hypersaline SW (Bagherie-Lachidan et al., 2008, 2009; Bui and Kelly, 2014; Gauberg et al., 2017). Thus, it is likely that increased Ocln abundance in the skin of IPW-acclimated ammocoetes contributed to a decrease in skin permeability. Similarly, Kwong and Perry (2013) related increased Ocln abundance with enhanced barrier function of larval zebrafish skin. An increase in *tric* transcript abundance was also noted in the skin of IPW-acclimated larvae, but was not mirrored by increased protein levels. A discrepancy between transcript and protein abundance of Tric has previously been reported in a cultured gill epithelium, where mRNA did not change but protein levels were elevated (Kolosov and Kelly, 2013). In the present study, increased mRNA abundance, with unchanged protein levels may be indicative of either (i) the onset of transcriptional upregulation or (ii) continuously fluctuating transcript and protein levels that happen to demonstrate opposing trends at the point of sampling. In either case, further investigation will be useful.

Ammocoete kidney

In the kidney of larval lamprey, *ocln*/Ocln and *ocln-a*/Ocln-a exhibited different responses following IPW acclimation. Specifically, an ∼15-fold increase in *ocln*, coupled with a threefold increase in Ocln was observed in IPW-acclimated lamprey. In contrast, *ocln-a* abundance was unaltered and Ocln-a significantly decreased in the kidney of IPW lamprey. In the stenohaline goldfish and *Xenopus laevis*, Ocln is postulated to be barrier forming in the nephron because of spatial differences in its distribution along the tissue. For example, goldfish Ocln-ir was not found in the proximal tubule of the nephron, but was strong to moderate at the apical membrane of renal epithelial cells lining the lumen of the distal tubule and collecting duct, respectively (Chasiotis and Kelly, 2008). Similarly, in the nephron of *X. laevis*, Ocln was undetectable in the proximal tubule but found at the apical membrane of distal tubule (early and late) and collecting duct renal epithelial cells (Chasiotis and Kelly, 2009). Because the proximal tubule of FW fishes is functionally 'leaky' compared with the distal tubule and collecting duct (for discussion, see Chasiotis and Kelly, 2008), the presence of Ocln in distal and collecting regions suggests it plays a barrier-forming role. Indeed, OCLN immunostaining patterns along the mammalian nephron suggest that 'tighter' epithelial segments have higher OCLN abundance than 'leakier' nephron regions (Kwon et al., 1998; González-

Journal of Experimental Biology (2017) 220, 3657-3670 doi:10.1242/jeb.161562

Mariscal et al., 2000). Given the challenge of retaining ions in IPW, it seems likely that increased *ocln*/Ocln abundance and decreased ocln-a/Ocln-a abundance in IPW-acclimated larval lamprey will contribute to ion retention and decreased water permeability.

Ammocoete GI tract

Differences in the spatial distribution of *ocln* and *ocln-a* were observed along the GI tract of larval lamprey, with *ocln-a* increasing towards the posterior and *ocln* exhibiting a modest but significant increase in the mid GI tract versus the anterior and posterior. Spatial differences in the distribution of *ocln* along the GI tract of other FW vertebrates have been reported (Chasiotis et al., 2010; Chasiotis and Kelly, 2009; Kelly and Chasiotis, 2011). In species such as the goldfish and *X. laevis*, greater *ocln* mRNA abundance has been observed in the posterior region of the GI tract (Chasiotis and Kelly, 2008, 2009) and observations of larval lamprey GI tract *ocln-a* distribution in the present study are consistent with this. This would suggest that the role of *ocln* in the GI tract of goldfish and *X. laevis* may be functionally similar to the role of *ocln-a* in larval lamprey. However, to our knowledge (and in the few species of aquatic vertebrate examined), no study has reported an elevation of *ocln* in the middle region of the GI tract. Transcript abundance of *tric* exhibited a stepwise increase from anterior to posterior in the GI tract of larval lamprey. This trend is also consistent with *tric* transcript abundance in the rainbow trout intestine, which increases substantially in the posterior region (Kolosov and Kelly, 2013). This would also suggest functional similarities between GI tract Tric in the lamprey and more derived fishes. But perhaps more importantly, regional differences in the transcript abundance of *ocln*, *ocln-a* and *tric* along the ammocoete GI tract, despite the absence of any clearly delineated functional anatomy, support the idea that the ammocoete gut exhibits spatial differences in permeability and barrier function.

In terms of how GI tract *ocln*, *ocln-a* and *tric* responded to IPW acclimation, no differences were observed in the anterior portion. In addition, *ocln-a* mRNA abundance did not change in other regions of the GI tract following IPW acclimation, suggesting that whatever role this TJ protein plays in the GI tract of larval lamprey, it was unperturbed following acclimation to IPW. In contrast, an appreciable reduction in *ocln* transcript abundance in the middle and posterior regions of ammocoete intestine was evident following IPW acclimation. These findings are in line with a previous study using stenohaline goldfish acclimated to IPW, where a similar decrease in Ocln abundance in the middle intestine occurred (Chasiotis et al., 2009). A decrease in TJ protein abundance has been proposed to be associated with increased paracellular permeability of the intestinal epithelium in order to facilitate passive ion uptake from food when it is present in the intestine (Scott et al., 2006). However, *tric* mRNA abundance increases in the middle GI tract of larval lamprey. To our knowledge, no study has examined whether and how IPW acclimation influences Tric in the GI tract of fishes, so the functional reason for this change will require further study. That said, *tric* mRNA abundance has been reported to increase in the middle intestine of Atlantic salmon acclimated from FW to SW (Tipsmark and Madsen, 2012). In this regard, the present study provides further evidence that water ion levels can have a regional influence on GI tract *tric* abundance in fishes.

Perspectives

Through the identification and characterization of Ocln isoforms and Tric in larval sea lamprey, the present study provides a first look at TJ-associated MARVEL proteins in a basal vertebrate. Evidence suggests that lamprey Ocln isoforms and Tric are found in the lamprey TJ complex, and that these proteins exhibit many similarities to the OCLN/Ocln and TRIC/Tric TJ proteins of derived vertebrates, including those of teleost fishes such as the goldfish (Chasiotis and Kelly, 2008) and rainbow trout (Chasiotis et al., 2010; Kolosov and Kelly, 2013). However, immunoelectron identification of lamprey TJ-associated MARVEL proteins is required to unequivocally define them as constituents of the sea lamprey TJ complex, and key distinctions also occur that suggest TJ-associated MARVEL proteins in this agnathan are regulated differently from those of gnathostomes. For example, what are the functional consequences of smaller protein spans in cytoplasmic N and C termini of lamprey MARVEL domain-containing proteins? Moreover, what functional differences occur between the two distinct lamprey Ocln isoforms? In the case of the latter, Ocln isoforms appear to collectively, but not individually, mirror the function of OCLN/Ocln in jawed vertebrates. This supports the idea that the function of OCLN/Ocln as we know it from derived chordates may be split between isoforms in less derived members of this phylum, or in this agnathan at least. Finally, although tricellular occluding proteins must have been around since epithelial cells formed tricellular complexes, finding a Tric in the lamprey genome dates the evolution of a major vertebrate tTJ protein to the agnathan/gnathostome split, providing insight into vertebrate tTJ protein evolution. Taken together, these results provide new insight into vertebrate TJ-associated MARVEL proteins and a foundation upon which future work on basal vertebrate TJ proteins can be built.

Acknowledgements

The α5 monoclonal antibody was developed by D. M. Fambrough and obtained from the Developmental Studies Hybridoma Bank (University of Iowa, Department of Biological Sciences, Iowa City, IA, USA). We thank Laura Tessier, Justine Doherty and Chris White at Wilfrid Laurier University, Waterloo, Ontario, for their assistance with the capture and transport of the sea lamprey used in this study.

Competing interests

The authors declare no competing or financial interests.

Author contributions

Conceptualization: D.K., S.P.K.; Methodology: D.K., A.D., S.P.K.; Formal analysis: D.K.; Investigation: D.K., P.B.; Resources: M.W., S.P.K.; Writing - original draft: D.K., S.P.K.; Writing - review & editing: D.K., P.B., A.D., M.W., S.P.K.; Supervision: S.P.K.; Project administration: S.P.K.; Funding acquisition: S.P.K.

Funding

This work was supported by Natural Sciences and Engineering Research Council of Canada Discovery Grants to S.P.K., A.D. and M.P.W. D.K. was supported by an Ontario Graduate Scholarship, Government of Ontario, followed by a York University Provost Dissertation Scholarship.

References

Bagherie-Lachidan, M., Wright, S. I. and Kelly, S. P. (2008). Claudin-3 tight junction proteins in *Tetraodon nigroviridis*: cloning, tissue-specific expression, and a role in hydromineral balance. *Am. J. Physiol. Integr. Comp. Physiol.* **294**, R1638-R1647.

Bagherie-Lachidan, M., Wright, S. I. and Kelly, S. P. (2009). Claudin-8 and -27 tight junction proteins in puffer fish *Tetraodon nigroviridis* acclimated to freshwater and seawater. *J. Comp. Physiol. B* **179**, 419-431.

Balda, M. S., Whitney, J. A., Flores, C., González, S., Cereijido, M. and Matter, K. (1996). Functional dissociation of paracellular permeability and transepithelial electrical resistance and disruption of the apical-basolateral intramembrane diffusion barrier by expression of a mutant tight junction membrane protein. *J. Cell Biol.* **134**, 1031-1049.

Bartels, H. and Potter, I. C. (1991). Structural changes in the zonulae occludentes of the chloride cells of young adult lampreys following acclimation to seawater. *Cell Tissue Res.* **265**, 447-457.

Bartels, H. and Potter, I. C. (1993). Intercellular junctions in the water-blood barrier of the gill lamella in the adult lamprey (*Geotria australis*, *Lampetra fluviatilis*). *Cell Tissue Res.* **274**, 521-532.

Bartels, H. and Potter, I. C. (2004). Cellular composition and ultrastructure of the gill epithelium of larval and adult lampreys: Implications for osmoregulation in fresh and seawater. *J. Exp. Biol.* **207**, 3447-3462.
Beamish, F. W. H. (1980). Osmoregulation in juvenile and adult lampreys. *Can. J. Fish. Aquat. Sci.* **37**, 1739-1750.
Bentley, P. J. (2002). *Endocrines and Osmoregulation: a Comparative Account in Vertebrates*. Berlin: Springer-Verlag.
Biazik, J. M., Thompson, M. B. and Murphy, C. R. (2007). The tight junctional protein occludin is found in the uterine epithelium of squamate reptiles. *J. Comp. Physiol. B* **177**, 935-943.
Bui, P. and Kelly, S. P. (2014). Claudin-6, -10d and -10e contribute to seawater acclimation in the euryhaline puffer fish *Tetraodon nigroviridis*. *J. Exp. Biol.* **217**, 1758-1767.
Chapman, J. A., Kirkness, E. F., Simakov, O., Hampson, S. E., Mitros, T., Weinmaier, T., Rattei, T., Balasubramanian, P. G., Borman, J., Busam, D. et al. (2010). The dynamic genome of *Hydra*. *Nature* **464**, 592-596.
Chasiotis, H. and Kelly, S. P. (2008). Occludin immunolocalization and protein expression in goldfish. *J. Exp. Biol.* **211**, 1524-1534.
Chasiotis, H. and Kelly, S. P. (2009). Occludin and hydromineral balance in *Xenopus laevis*. *J. Exp. Biol.* **212**, 287-296.
Chasiotis, H., Effendi, J. C. and Kelly, S. P. (2009). Occludin expression in goldfish held in ion-poor water. *J. Comp. Physiol. B* **179**, 145-154.
Chasiotis, H., Wood, C. M. and Kelly, S. P. (2010). Cortisol reduces paracellular permeability and increases occludin abundance in cultured trout gill epithelia. *Mol. Cell. Endocrinol.* **323**, 232-238.
Chasiotis, H., Kolosov, D., Bui, P. and Kelly, S. P. (2012a). Tight junctions, tight junction proteins and paracellular permeability across the gill epithelium of fishes: a review. *Resp. Physiol. Neurobiol.* **184**, 269-281.
Chasiotis, H., Kolosov, D. and Kelly, S. P. (2012b). Permeability properties of the teleost gill epithelium under ion-poor conditions. *Am. J. Physiol. Regul. Integr. Comp. Physiol.* **302**, R727-R739.
Chen, Y., Merzdorf, C., Paul, D. L. and Goodenough, D. A. (1997). COOH terminus of occludin is required for tight junction barrier function in early *Xenopus* embryos. *J. Cell Biol.* **138**, 891-899.
Chen, C. C., Kolosov, D. and Kelly, S. P. (2016). The liquorice root derivative glycyrrhetinic acid can ameliorate ionoregulatory disturbance in rainbow trout (*Oncorhynchus mykiss*) abruptly exposed to ion-poor water. *Comp. Biochem. Physiol. A* **199**, 120-129.
Chishti, M. S., Bhatti, A., Tamim, S., Lee, K., McDonald, M.-L., Leal, S. M. and Ahmad, W. (2008). Splice-site mutations in the TRIC gene underlie autosomal recessive nonsyndromic hearing impairment in Pakistani families. *J. Hum. Genet.* **53**, 101-105.
Donini, A. and O'Donnell, M. J. (2005). Analysis of Na^+, Cl^-, K^+, H^+ and NH_4^+ concentration gradients adjacent to the surface of anal papillae of the mosquito *Aedes aegypti*: application of self-referencing ion-selective microelectrodes. *J. Exp. Biol.* **208**, 603-610.
Dörfel, M. J., Westphal, J. K., Bellmann, C., Krug, S. M., Cording, J., Mittag, S., Tauber, R., Fromm, M., Blasig, I. E. and Huber, O. (2013). CK2-dependent phosphorylation of occludin regulates the interaction with ZO-proteins and tight junction integrity. *Cell. Commun. Signal.* **11**, 40.
Duffy, N. M., Bui, P., Bagherie-Lachidan, M. and Kelly, S. P. (2011). Epithelial remodeling and claudin mRNA abundance in the gill and kidney of puffer fish (*Tetraodon biocellatus*) acclimated to altered environmental ion levels. *J. Comp. Physiol. B* **181**, 219-238.
Evans, D. H., Piermarini, P. M. and Choe, K. P. (2005). The multifunctional fish gill: dominant site of gas exchange, osmoregulation, acid-base regulation, and excretion of nitrogenous waste. *Physiol. Rev.* **85**, 97-177.
Farquhar, M. G. and Palade, G. E. (1963). Junctional complexes in various epithelia. *J. Cell Biol.* **17**, 375-412.
Feldman, G. J., Mullin, J. M. and Ryan, M. P. (2005). Occludin: structure, function and regulation. *Adv. Drug Deliv. Rev.* **57**, 883-917.
Furuse, M., Hirase, T., Itoh, M., Nagafuchi, A., Yonemura, S., Tsukita, S. and Tsukita, S. (1993). Occludin: a novel integral membrane protein localizing at tight junctions. *J. Cell Biol.* **123**, 1777-1788.
Furuse, M., Itoh, M., Hirase, T., Nagafuchi, A., Yonemura, S., Tsukita, S. and Tsukita, S. (1994). Direct association of occludin with ZO-1 and its possible involvement in the localization of occludin at tight junctions. *J. Cell Biol.* **127**, 1617-1626.
Furuse, M., Sasaki, H., Fujimoto, K. and Tsukita, S. (1998). A single gene product, claudin-1 or -2, reconstitutes tight junction strands and recruits occludin in fibroblasts. *J. Cell Biol.* **143**, 391-401.
Furuse, M., Izumi, Y., Oda, Y., Higashi, T. and Iwamoto, N. (2014). Molecular organization of tricellular tight junctions. *Tissue Barriers* **2**, e28960.
Gauberg, J., Kolosov, D. and Kelly, S. P. (2017). Claudin tight junction proteins in rainbow trout (*Oncorhynchus mykiss*) skin: Spatial response to elevated cortisol levels. *Gen. Comp. Endocrinol.* **240**, 214-226.
González-Mariscal, L., Namorado, M. C., Martin, D., Luna, J., Alarcon, L., Islas, S., Valencia, L., Muriel, P., Ponce, L. and Reyes, J. L. (2000). Tight junction proteins ZO-1, ZO-2, and occludin along isolated renal tubules. *Kidney Int.* **57**, 2386-2402.
Günzel, D. and Fromm, M. (2012). Claudins and other tight junction proteins. *Compr. Physiol.* **2**, 1819-1852.
Hardisty, M. W. (1956). Some aspects of osmotic regulation in lampreys. *J. Exp. Biol.* **33**, 431-447.
Ikenouchi, J., Furuse, M., Furuse, K., Sasaki, H., Tsukita, S. and Tsukita, S. (2005). Tricellulin constitutes a novel barrier at tricellular contacts of epithelial cells. *J. Cell Biol.* **171**, 939-945.
Karnaky, K. J., Jr. (2001). Teleost chloride cell tight junctions: environmental salinity and dynamic structural changes. In *Tight Junctions*, 2nd edn (ed. M. Cereijido and J. Anderson), pp. 445-458. Boca Raton, FL: CRC Press.
Kelly, S. P. and Chasiotis, H. (2011). Glucocorticoid and mineralocorticoid receptors regulate paracellular permeability in a primary cultured gill epithelium. *J. Exp. Biol.* **214**, 2308-2318.
Kluge, B. and Fischer, A. (1991). The pronephros of the early ammocoete larva of lampreys (Cyclostomata, Petromyzontes): fine structure of the renal tubules. *Cell Tissue Res.* **263**, 515-528.
Kolosov, D. and Kelly, S. P. (2013). A role for tricellulin in the regulation of gill epithelium permeability. *Am. J. Physiol. Regul. Integr. Comp. Physiol.* **304**, R1139-R1148.
Kolosov, D. and Kelly, S. P. (2016). Dietary salt loading and ion-poor water exposure provide insight into the molecular physiology of the rainbow trout gill epithelium tight junction complex. *J. Comp. Physiol. B* **186**, 739-757.
Kolosov, D., Bui, P., Chasiotis, H. and Kelly, S. P. (2013). Claudins in teleost fishes. *Tissue Barriers* **1**, e25391.
Kolosov, D., Chasiotis, H. and Kelly, S. P. (2014). Tight junction protein gene expression patterns and changes in transcript abundance during development of model fish gill epithelia. *J. Exp. Biol.* **217**, 1667-1681.
Korompay, A., Borka, K., Lotz, G., Somorácz, Á., Törzsök, P., Erdélyi-Belle, B., Kenessey, I., Baranyai, Z., Zsoldos, F., Kupcsulik, P. et al. (2012). Tricellulin expression in normal and neoplastic human pancreas. *Histopathol.* **60**, E76-E86.
Krug, S. M., Amasheh, S., Richter, J. F., Milatz, S., Günzel, D., Westphal, J. K., Huber, O., Schulzke, J. D. and Fromm, M. (2009). Tricellulin forms a barrier to macromolecules in tricellular tight junctions without affecting ion permeability. *Mol. Biol. Cell* **20**, 3713-3724.
Krug, S. M., Amasheh, M., Dittmann, I., Christoffel, I., Fromm, M. and Amasheh, S. (2013). Sodium caprate as an enhancer of macromolecule permeation across tricellular tight junctions of intestinal cells. *Biomaterials* **34**, 275- 282.
Kwon, O., Myers, B. D., Sibley, R., Dafoe, D., Alfrey, E. and Nelson, W. J. (1998). Distribution of cell membrane-associated proteins along the human nephron. *J. Histochem. Cytochem.* **46**, 1423-1434.
Kwong, R. W. M. and Perry, S. F. (2013). Cortisol regulates epithelial permeability and sodium losses in zebrafish exposed to acidic water. *J. Endocrinol.* **217**, 253-264.
Marshall, W. S. and Grosell, M. (2006). Ion transport, osmoregulation, and acid-base balance. In *The Physiology of Fishes*, 3rd edn (ed. D. H. Evans and J. B. Claiborne), pp. 177-210. Boca Raton, FL: Taylor and Francis Group.
Morris, R. (1980). Blood composition and osmoregulation in ammocoete larvae. *Can. J. Fish. Aquat. Sci.* **37**, 1665-1679.
Ohkuni, T., Kojima, T., Ogasawara, N., Masaki, T., Ninomiya, T., Kikuchi, S., Go, M., Takano, K.-I., Himi, T. and Sawada, N. (2009). Expression and localization of tricellulin in human nasal epithelial cells *in vivo* and *in vitro*. *Med. Mol. Morphol.* **42**, 204-211.
Parry, G. (1966). Osmotic adaptation in fishes. *Biol. Rev. Camb. Philos. Soc.* **41**, 392-440.
Peek, W. D. and Youson, J. H. (1979). Transformation of the interlamellar epithelium of the gills of the anadromous sea lamprey, *Petromyzon marinus* L., during metamorphosis. *Can. J. Zool.* **57**, 1318-1332.
Perry, S. F. and Laurent, P. (1989). Adaptational responses of rainbow trout to lowered external NaCl concentration: contribution of the branchial chloride cell. *J. Exp. Biol.* **147**, 147-168.
Raleigh, D. R., Marchiando, A. M., Zhang, Y., Shen, L., Sasaki, H., Wang, Y., Long, M. and Turner, J. R. (2010). Tight junction-associated MARVEL proteins marveld3, tricellulin, and occludin have distinct but overlapping functions. *Mol. Biol. Cell* **21**, 1200-1213.
Riazuddin, S., Ahmed, Z. M., Fanning, A. S., Lagziel, A., Kitajiri, S. I., Ramzan, K., Khan, S. N., Chattaraj, P., Friedman, P. L., Anderson, J. M. et al. (2006). Tricellulin is a tight-junction protein necessary for hearing. *Am. J. Hum. Genet.* **79**, 1040-1051.
Saitou, M., Ando-Akatsuka, Y., Itoh, M., Furuse, M., Inazawa, J., Fujimoto, K. and Tsukita, S. (1997). Mammalian occludin in epithelial cells: its expression and subcellular distribution. *Eur. J. Cell Biol.* **73**, 222-231.
Schlüter, H., Moll, I., Wolburg, H. and Franke, W. W. (2007). The different structures containing tight junction proteins in epidermal and other stratified epithelial cells, including squamous cell metaplasia. *Eur. J. Cell Biol.* **86**, 645-655.
Scott, G. R., Schulte, P. M. and Wood, C. M. (2006). Plasticity of osmoregulatory function in the killifish intestine: drinking rates, salt and water transport, and gene expression after freshwater transfer. *J. Exp. Biol.* **209**, 4040-4050.

Smith, J. J., Kuraku, S., Holt, C., Sauka-Spengler, T., Jiang, N., Campbell, M. S., Yandell, M. D., Manousaki, T., Meyer, A., Bloom, O. E. et al. (2013). Sequencing of the sea lamprey (*Petromyzon marinus*) genome provides insight into vertebrate evolution. *Nat. Genet.* **45**, 415-421.

Tipsmark, C. K. and Madsen, S. S. (2012). Tricellulin, occludin and claudin-3 expression in salmon intestine and kidney during salinity adaptation. *Comp. Biochem. Physiol. A* **162**, 378-385.

Wetzel, R. G. (1983). *Limnology*, 2nd edn. Philadelphia, PA: Saunders College Publishing.

Wilkie, M. P., Wang, Y., Walsh, P. J. and Youson, J. H. (1999). Nitrogenous waste excretion by the larvae of a phylogenetically ancient vertebrate: the sea lamprey (*Petromyzon marinus*). *Can. J. Zool.* **77**, 707-715.

Zydlewski, J. and Wilkie, M. P. (2013). Freshwater to seawater transitions in migratory fishes. In *Fish Physiology*, Vol. 32 (ed. S. D. McCormick, A. P. Farrell and C. J. Brauner), pp. 254-294. Oxford: Academic Press.